Some Recent Advances in Nonlinear Aeroelasticity: Fluid-Structure Interaction in the 21st Century

Earl H. Dowell[1]
Duke University, Durham, NC 27708

Aeroelasticity is the field that examines, models and seeks to understand the interaction of the forces from an aerodynamic flow and the deformation of an elastic structure. The forces produce deformation, but the structural deformation in turn changes the aerodynamic forces. This feedback between force and deformation leads to a variety of dynamic responses of the fluid and the structure including flutter (a Hopf bifurcation), limit cycle oscillations and sometimes chaos. Selected recent advances in nonlinear aeroelasticity and fluid-structure interaction are reviewed to identify and model the fundamental elements that they share. Topics discussed include the following.

Transonic and Subsonic Panel Flutter
Freeplay Induced Flutter and Limit Cycle Oscillations (LCO)
Reduced Order Modeling (ROM) of Unsteady Aerodynamics
  Eigenmodes and POD Modes
  High Dimensional Harmonic Balance (HDHB)
  Nonlinear ROM based upon POD and HDHB
Transonic Flutter and LCO of Lifting Surfaces
  Flight Experience
  Efficient and Accurate Computation of Aerodynamic Forces
  Experimental/Theoretical Correlations
Aerodynamic LCO: Buffet, Abrupt Wing Stall and Non-Synchronous Vibration

I. Introduction

SOME twenty plus years ago I had the pleasure of giving the SDM lecture in Mobile, Alabama and am happy to have the opportunity to do so again here in Orlando. When asked to give this SDM lecture, I mentioned my previous experience and suggested that being asked to do so again might be considered double jeopardy. But I was assured that no one would remember my earlier talk!

However, I do recall that twenty years ago a then radical idea was discussed in the lecture, i.e. that one could use the eigenmodes of an aerodynamic flow to construct a modal model of the flow much as has been done for many years for structures. Whether that suggestion inspired anyone other than our group at Duke, I cannot be sure. But in any event, reduced order modeling of flow fields and their interaction with structural response is today a flourishing topic. Indeed reduced order modeling is now pervasive in many fields of engineering and science, no doubt having been discovered and rediscovered many times by many investigators. And the topic has been generalized in at least three significant ways that I will discuss in this lecture. Given the title of this lecture you will not be surprised that one of the generalizations is to treat the *nonlinear as well as linear dynamics of aeroelastic or fluid-structural systems.* Thus the major theme of this talk is the modeling of nonlinear aeroelastic systems both mathematically and computationally as well as experimentally.

II. Motivation and Goals

The motives for pursuing research and developing methods that are useful in practice are many. But to provide a context and rationale for much of the work to be described in this lecture, perhaps a few words about goals will be helpful.

When my contemporaries and I first began the study and practice of aeroelasticity, and for a number of years thereafter, any difference between theory and experiment of design and reality was often attributed to nonlinear effects. However, it was generally understood that trying to model such *nonlinear effects* was not to be expected or

[1] William Holland Hall Professor, Mechanical Engineering, P.O. Box 90300, Fellow

attempted. Since then many studies of nonlinear effects have been undertaken and today the subject is treated in review articles [1-4] and indeed in textbooks [5,6]. An engineer today no longer has the luxury of simply ignoring such effects and one of my predictions is that some years from now an SDM Lecturer will be discussing the favorable effects that can be created by a judicious analysis and design of nonlinearities in aeroelastic systems. Of course there are unfavorable and indeed potentially catastrophic consequences of nonlinearities in aeroelastic systems as well, as is also the case when an aeroelastic system is analyzed and designed with linear models.

The motivation for *reduced order modeling* is much the same for fluid systems as for structural systems. In either case, a relative small number of modes is often (but not always!) sufficient to describe the dynamics of a structural or fluid system. In the case of a structure an initial mathematical/computational model may consist of a finite element representation with several thousand degrees of freedom while for a computational fluid dynamics (CFD) model there may be millions of degrees of freedom. If one can use say one hundred modes or less to describe the structure or the fluid, then clearly there is a great potential for savings in the cost of the computation. Indeed at any given point in time of the state of the art in computer hardware and software, there will be computations that are only feasible if one uses a reduced order model.

But here it is worth noting that another very important advantage of reduced order models is the greater physical insight they may give to the investigator. While a dynamical system with one hundred degrees of freedom or less may be still one of considerable complexity, it pales in complexity compared to a system with thousands not to mention millions of degrees of freedom. Moreover it is often the case that the response of the aeroelastic system is governed by an even smaller number of modes than the structural or fluid system individually. This is because the fluid and structural modes of greatest interest will be those that match most closely in both the spatial (wavelength) and temporal (frequency) domains. In the field of acoustics this matching of frequency and wavelength is called "coincidence." Lest one think this means that reduced order models may be smaller than in fact they reasonably can be, it is well to point out two important facts. First, it cannot always be anticipated which fluid and structural modes will be most important for an aeroelastic system and thus more modes must be retained than would otherwise be the case (once the most dominant aeroelastic modes are determined!).Secondly, if one wishes to control or modify the aeroelastic system, some of the fluid, structural, and/or aeroelastic or coupled fluid-structural modes that may not have been important before can now become important. Therefore and again, more modes must be retained as control of the system is considered.

It is sometimes said that the use of modes is only possible for a linear system. It is now widely, though not universally, appreciated that modes can be used for nonlinear systems as well. Having said that, for linear systems the use of eigenmodes is almost always the preferred choice for constructing a reduced order model. But for nonlinear systems other choices of modes may be preferred, e.g. the modes that can be constructed from Proper Orthogonal Decomposition, so called POD modes. These modes have been used very successfully by Dowell and colleagues at Duke, Beran and colleagues at the Air Force Research Laboratory (AFRL) and by Farhat and colleagues at Stanford.

Finally, one can think of modes as a form of generalized Fourier series in the spatial domain. Therefore it is perhaps not surprising that a Fourier Series in time can also be very useful if the temporal response is periodic. As was the case for eigenmodes versus POD modes for the representation of the spatial domain of nonlinear systems, for nonlinear systems a standard Fourier Series or classical Harmonic Balance method may not be the best choice for describing the temporal response. The Higher Order Harmonic Balance method developed by Hall and his colleagues at Duke has proven to be a very effective method and it has now also been adopted and exploited by Jameson and colleagues at Stanford and Badcock and colleagues at Liverpool. A related method has also been developed by Beran and colleagues at AFRL.

The remainder of the paper is organized as follows. In Section III.A transonic panel flutter and the effect of a viscous boundary layer is treated, in Section III.B the structural nonlinearity of freeplay and its effect on flutter and limit cycle oscillations (LCO) is discussed, in Section III.C reduced order modeling is summarized, in Section IV transonic flutter and LCO of lifting surfaces is reviewed and, finally, in Section V aerodynamic limit cycle oscillations are discussed, e.g. buffet, abrupt wing stall and non-synchronous vibration. The present discussion is not meant to be exhaustive of the study of either nonlinear aeroelasticity or the reduced order modeling. For example, the nonlinear aeroelasticity of very high aspect ratio, flexible wings is not treated here (for an introduction to that topic, see [2]) or the use of Volterra series for reduced order modeling (for an introduction to that topic see [4]). Also rotorcraft and turbomachinery aeroelasticity, morphing aircraft and other important topics are not treated here, but are nonetheless active areas of research as seen in papers at this SDM conference. The topics that have been chosen for this paper are representative of the active and productive work underway and are those for which the present author can claim some personal experience.

III. Current Examples of Recent Advances

A. Transonic and Subsonic Panel Flutter

Although the vast majority of the literature on panel flutter analysis is devoted to high supersonic/hypersonic flow, many of the flutter incidents in practice have occurred in the low supersonic/transonic Mach number regime. A recent paper by Hashimoto, Aoyama and Nakamura [7] provides new insight into the importance of a viscous fluid boundary layer on the transonic flutter boundary. Previous work by Dowell [8] had shown this effect as well. But whereas Dowell used what is sometimes called a shear flow model that dates back to work of Lighthill and others, the more recent work of Hashimoto et al uses a modern CFD code that solves the Navier-Stokes equations within the framework of a Reynolds Averaged Navier-Stokes model. The shear flow model by contrast uses a mean flow that represents the boundary layer, but neglects the viscosity in the small perturbation equations of the fluid that arise from the panel oscillation. The more rigorous fluid model shows improved agreement with the excellent experiments of Muhlstein, Gaspers and Riddle [9].

Figure 1 is a schematic of the panel and flow geometry. Figure 2 shows the comparison between theory and experiment where the experimental data have been extrapolated to zero boundary layer thickness, $\delta/a = 0$, where δ is the boundary layer thickness and a is the panel length. The theoretical results from Dowell are for transonic potential flow and those from Hashimoto et al are for inviscid Euler flow. The plot is of a non-dimensional dynamic pressure versus Mach number. The good agreement among all results is encouraging. Turning now to the case for a boundary layer thickness of $\delta/a = .1$, a similar comparison is shown in Figure 3. Note that the flutter boundary predicted by theory and that determined experimentally has been very substantially changed from that for $\delta/a = 0$, especially in the lower Mach number range. The dynamic pressure for flutter at M = 1.1 has been increased by a factor of 2-3 due to the viscous boundary layer. While the shear flow model used by Dowell is a substantial improvement over an inviscid analysis that neglects the boundary layer effect, the RANS flow model of Hashimoto et al is a notable further improvement and agrees better with experiment.

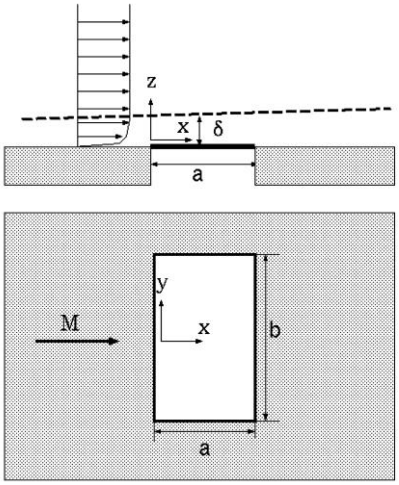

Figure 1: Schematics of Panel Flutter Problem

Moreover, as Hashimoto et al note this is an excellent test case for new developments in CFD methodology for aeroelastic analysis in general and gives considerable confidence in the basic theory. They have also shown that in this particular case the results are not sensitive to the empirical turbulence model used in the RANS flow model.

While subsonic panel flutter is unusual in aerospace applications it has been known for many years that panel flutter may occur at subsonic conditions under some circumstances [10]. Most notably if the trailing edge of the

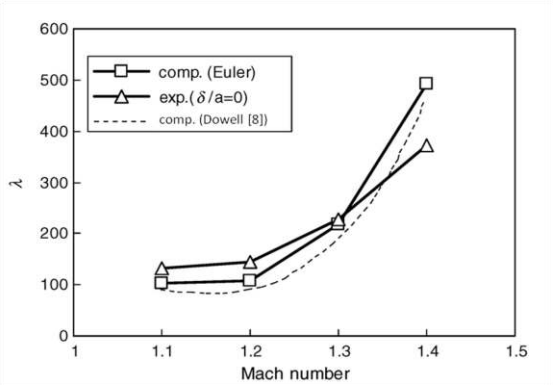

Figure 3: Flutter Boundary (Inviscid Case)

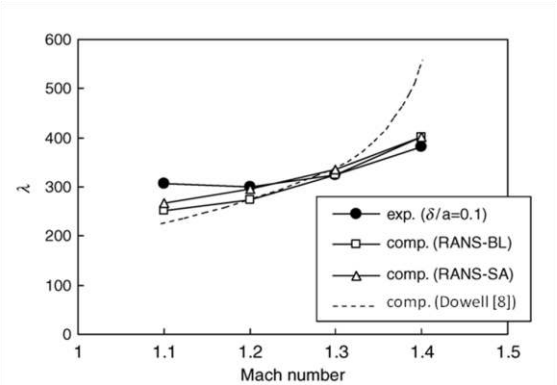

Figure 2: Flutter Boundary (Viscous Case)

panel is free, then flutter will occur in subsonic flow. But, if the trailing edge, as well as the leading edge, of the panel is fixed then divergence (a static aeroelastic instability) will occur rather than flutter. Panel divergence is a form of aeroelastic buckling and, when the panel is in a buckled state, then oscillations in the flow due for example to engine or boundary layer noise may cause a buckled panel to " oil can" from one buckled state to another. This is

sometimes referred to as "dynamic buckling" [10]. In experiments as well as in nonlinear numerical simulations it may be difficult to distinguish between limit cycle oscillations due to flutter and oil canning due to dynamic buckling.

The classical example of subsonic panel flutter was described in the paper by Dugundji and colleagues [11] who considered a panel on an elastic foundation that can lead to a form of traveling wave flutter. Here recent work on subsonic flutter is emphasized. See [12,13]. The work of Tang, Yamamoto and Dowell [12] is for a panel clamped at its leading edge, but free on both side edges and, most importantly, free on its trailing edge. Both theoretical and experimental work has been done and the agreement between theory and experiment is very good for the prediction of flutter flow velocity and frequency. However, in the experiments, hysteresis is observed that this is not predicted by the theory which includes a nonlinear structural model and a nonlinear vortex lattice aerodynamic model [12,13]. Moreover the amplitude of the limit cycle oscillation (LCO) that is observed in the experiment after the onset of flutter and indeed at lower flow velocities due to hysteresis is some two to three times greater than that predicted by the theoretical model. Currently the most plausible hypothesis for the differences between theory and experiment is that vortex shedding and flow separation may occur at the large amplitudes of the LCO. These effects are not included in the vortex lattice aerodynamic model, but would be included in a viscous flow model based upon the Navier-Stokes equations.

Because the LCO amplitudes are on the order of the panel chord (LCO amplitudes of panels which are fixed on two opposing edges are typically much smaller and on the order of the panel thickness [11]), Tang, Paidoussis and Jiang [13] have suggested such a LCO is a prime candidate for energy harvesting. And they have analyzed this configuration inter alia using a similar theoretical model and obtained similar results.

Figure 4 shows a stroboscopic picture of the panel in LCO during a wind tunnel test [12]. Note the amplitude of the LCO relative to the panel chord.

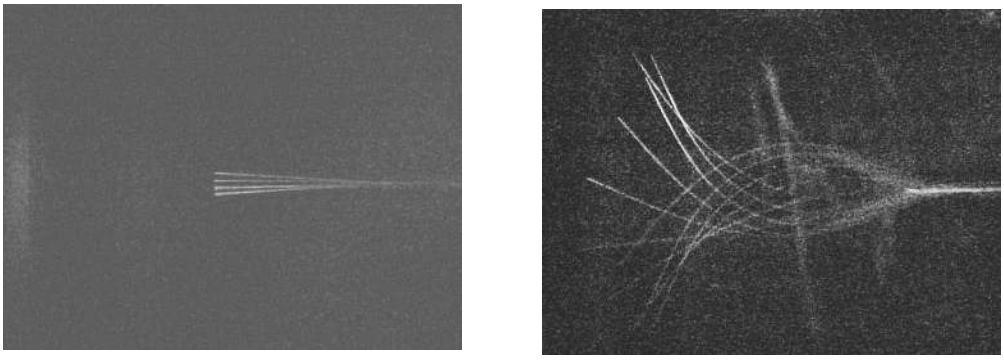

Figure 4: Flutter oscillations of an elastic panel with a clamped leading edge and all other edges free. Subsonic flow is from right to left.

This configuration is also an example of what is sometimes referred to as "flag flutter", but here the bending stiffness of the panel is dominant over the tension/membrane stiffness of the panel where the latter might be induced by gravity or shear stresses produced by a viscous flow. So this is a rather stiff "flag". Current applications to micro airvehicles and coverings for gaps in conventional wing/control surfaces during landing may give rise to renewed interest in subsonic panel flutter for panels and/or thin membranes where both the bending stiffness and membrane stiffness may be important.

B. Freeplay Induced Flutter and Limit Cycle Oscillations

Freeplay is a concern with respect to control surface attachments, but it has also been suggested as a possible source of flutter and limit cycle oscillations in wing/store attachments. The latter is still an open area of investigation, but recent progress for freeplay in control surfaces offers an opportunity to enhance both analysis and design methods and may lead to a paradigm shift in design criteria.

Here a brief review of history is provided, the results of recent advances in understanding based upon computations and wind tunnel testing are summarized and the current design criteria and the data on which they are based are reinterpreted in light of recent advances.

Figure 5 is taken from one of a series of early reports [14] on the effect of freeplay on control surface flutter and limit cycle oscillations (LCO) conducted at the Wright Air Development Center, the predecessor to the Air Force

Research Laboratory. It is plot of the putative flutter velocity versus the total angular freeplay in an all movable control surface. The relevant conclusions drawn at that time from these data were the following.

"The test data also show the variation in flutter speed as a function of free-play...."

"Free-play in all movable controls should be limited to + or - 1/64 degrees unless it can be shown by means of experimental flutter model data that reasonable deviations from this free-play limit can be tolerated for the particular all-movable control design being considered."

This limit of + or - 1/64 degrees remains today more than fifty years later as the basic design criterion to preclude freeplay induced flutter (and limit cycle oscillations).

Recent computational and experimental work [15-18] has shed new light on these earlier results. It is now understood that in fact, for an unloaded control surface, the flow velocity at which limit cycle oscillations (LCO) begins is *independent* of the degree of freeplay. Note that even in Figure 5 the early tests concluded that the flutter velocity was independent of the freeplay angle as this angle became large.

However, it is now known that the amplitude of the LCO and the amount of loading required to preclude LCO is strongly dependent on the degree of freeplay. In fact the LCO amplitude scales in proportion to the degree of freeplay and the amount of loading required to suppress flutter/LCO does as well. For example, the LCO amplitude will be of the order of the degree of freeplay and if the loading is due to placing the airfoil at an angle of attack, the angle of attack required to totally eliminate freeplay is about five times the degree of freeplay. Thus for a freeplay of 1/64 degrees the LCO amplitude will be about 1/64 degrees and an angle of attack of 5/64 degrees is sufficient to suppress the LCO altogether. This then likely explains the apparent variation of the flutter speed with freeplay angle shown in Figure 5 from the earlier tests. For small freeplay angles, it is likely the LCO amplitude was undetectable and/or unavoidable small amounts of angle of attack were sufficient to load the wing so that LCO was suppressed.

More recent investigations by Tang and Dowell [15,16], Lee et al [17] and Schlomach [18] have confirmed the effect of freeplay and loading on LCO. Figures 6 (full model view) and 7 (close up of the wire beam that moves between two rigid stops to produce freeplay) show the wind tunnel model from [11-13]. Figure 8 shows the LCO amplitude of the model versus flow velocity for plunge, pitch and flap (control surface) degrees of freedom of this model as well as the LCO frequency. Note the computational results are in very good agreement with the wind tunnel test data. These results are for zero angle of attack and a freeplay angle of 2.12 degrees. If the angle of attack is increased to 8 degrees, as shown in Figure 9 the range of flow velocity for which LCO exists is much decreased and a further increase in angle of attack to 10 degrees suppresses the LCO altogether. Note however that the flow velocity at which the LCO begins is not much changed by the angle of attack change. Results (not shown) also show that varying the degree of freeplay simply changes the LCO amplitude in proportion while the LCO frequency is unchanged [15-17].

Current work is underway to include the effect of a feedback control system in this model.

The excellent work of Schlomach [18] for the F-35 program has provided independent verification of the above results and extended them into the high subsonic/transonic flow regime. As expected the quantitative agreement between theory and experiment is less satisfactory in the transonic regime because of the challenging environment for modeling the aerodynamic forces. However, even so, the same scaling laws for the effect of freeplay and loading were also found in this study.

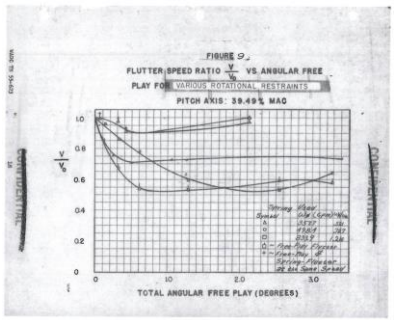

Figure 5: Flutter Velocity Versus Freeplay

Figure 6: Photograph of the Experimental Model with Gust Generator in the Wind Tunnel Test

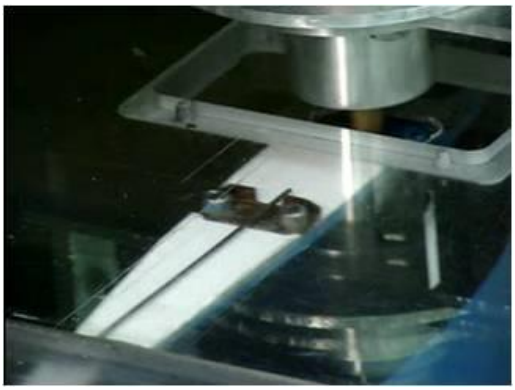

Figure 7: Close-Up of Freeplay Mechanism

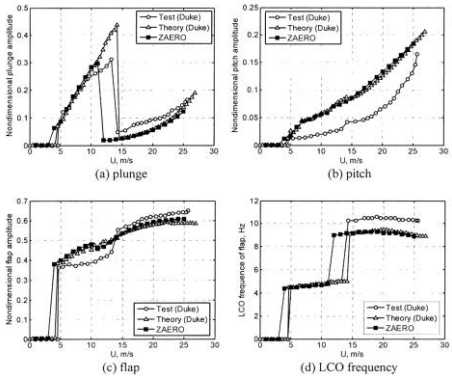

Figure 8: Theoretical and Experimental LCO R.M.S. Response Amplitudes and Frequency for the Initial Pitch Angles of α=0 and δ=2.12°

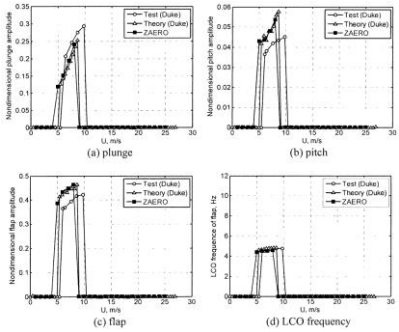

Figure 9: Theoretical and Experimental LCO R.M.S. Response Amplitudes and Frequency for the Initial Pitch Angles of $\alpha_0 = 8^0$ and δ=2.12°

C. Reduced Order Modeling of Unsteady Aerodynamics

For an expanded discussion and reviews of this topic, see [1-6].

1. Eigenmodes and POD Modes:

The original impetus for such models was the thought that by using the eigenmodes of a computational fluid dynamics (CFD) model, one might construct a modal model of the fluid that is the counterpart for the modal model of a structure obtained from a finite element model (FEM). [1-6] And this turns out to be possible with some notable caveats. First of all, finding the eigenmodes of a CFD model is itself a formidable task because of the very large number of degrees of freedom in a typical CFD model. And indeed the use of Proper Orthogonal Decomposition (POD) to find a suitable set of fluid modes proves to be far more practical. However it is worth noting in passing that using POD modes one may find a good approximation to the dominant eigenmodes of a CFD model. Normally however one uses the POD modes themselves in an aeroelastic analysis. [3]

Also it is worth noting that the fluid modal model is non-self adjoint and thus the fluid eigenvalues are complex with each fluid mode eigenvalue having both a frequency and a damping. Thus both the system and its adjoint must be considered when constructing the orthogonality relations for the complex eigenmodes. And perhaps most importantly, the eigenmodes and the POD modes can be very sensitive to small changes in system parameters, most notably there is a sensitivity to Mach number. Thus when using POD modes it is most convenient to fix the Mach number and vary the altitude or flow density for example. However Farhat [19-21] and his colleagues have made very good progress in showing how one may interpolate POD modes obtained at two different Mach numbers to obtain a good ROM model at intermediate Mach numbers thereby expanding the range of application of such ROMs. This interpolation proves to be surprisingly subtle.

For a chronological development of this approach including the seminal paper by Romanowski [22], the reader may consult [22-29]. There is a discussion of the eigenmode and/or POD mathematical technique in most of these papers and readily accessible accounts are available in [3-6].

2. High Dimensional Harmonic Balance

Here the essential idea is that most aeroelastic responses of interest are periodic in time. As those who have tried to compute the periodic in time limit cycle oscillation (LCO) using a time marching CFD code have observed, it takes a very long time to do so while waiting for the transient oscillation to decay in order to reach the steady state LCO. Indeed at the flutter point in parameter space which is usually the point at which LCO also begins, the damping in the critical aeroelastic mode is strictly speaking zero and the transient never decays. But even near the flutter point, the transients are usually very long.

Thus it is natural to ask can one avoid computing the transient solution and compute the LCO directly. Classical Harmonic Balance has been used successfully in pursuit of this goal for low dimensional systems, e.g. the Duffing

and Van der Pol oscillators. However for the high dimensional systems of interest using a nonlinear CFD model, the classical method becomes practically impossible. Thus Hall and colleagues [3] developed a significant extension to the classical Harmonic Balance method that is particularly useful for high dimensional dynamical systems such as those arising from CFD models. Other investigators have found this approach useful as well. See the work of Jameson et al [30,31] and Badcock [32].

For a chronological development of this approach including the seminal paper by Hall, Thomas and Clark [33], see [33-39]. For an accessible account of the mathematical formulation of the High Dimensional Harmonic Balance method, see [34,40]. Beran and Lucia [35] have developed a related approach that has some interesting alternative ideas.

For systems that are not strictly periodic in time, but have two fundamental periods or frequencies, the classical and Higher Order Harmonic Balance Methods can also be useful if a Fourier Series for each period is constructed. If the system is nonlinear then the coupling between the (as well as within each of the) components of the two Fourier Series must be taken into account. While a system with only two fundamental periods may be thought to be rather limited from a mathematical point of view, in point of fact it includes systems of interest to aeroelasticians, e.g. an aeroelastic system undergoing a limit cycle oscillation of a certain period or frequency which is then excited by an external dynamic force such as a gust with its own characteristic frequency.

3. Nonlinear Reduced Order Models Based Upon POD Modes and High Dimensional Harmonic Balance

Thomas, Dowell and Hall [40] have recently combined the advantages of POD modes and High Dimensional Harmonic Balance to construct *nonlinear* reduced order models. In this approach, the solution is expanded in a Taylor Series with respect to CFD code parameters including variables such as Mach and the amplitude of the structural motion. If this expansion were done for each of the many fluid variable degrees of freedom that may number in the millions or more, the computation would quickly get out of hand. However if one relates the many flow variables through a coordinate transformation to the modal amplitudes of a relatively small number of POD modes, then the computational model can be made very efficient. The key then is to be able to differentiate the CFD code and its flow variables with respect to the POD modal amplitudes and this can be accomplished using adjoint automatic differentiation software that is now widely available [40]. In [40] this reduced order model is constructed in combination with a High Dimensional Harmonic Balance (HDHB) solver. In principle this POD approach could also be combined with a time marching solution algorithm, but that would not exploit the considerable advantages of the HDHB method.

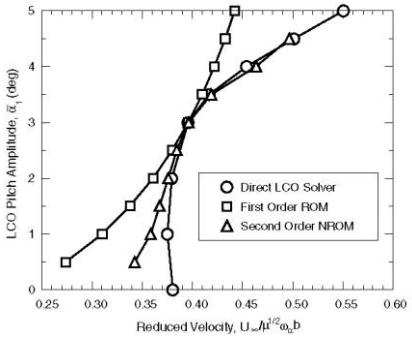

Figure 10: LCO Response Trends for the NLR 7301 Aeroelastic Configuration Including Reduced-Order-Model Results

A representative result [40] is shown in Figure 10 where the results of the full CFD model and the reduced order model (ROM) are compared in a plot of LCO amplitude versus a reduced (non-dimensional) velocity. Results are shown for both a first and second order ROM. As can be seen the second order ROM is a distinct improvement over the first order ROM. Of course in principal one can go to a third order ROM etc. However in practice a better strategy is to choose a small number of full order solutions and expand in a Taylor Series up to say second order about each of them. Referring to Figure 10, it is seen that the common point on the three curves is the point about which the Taylor Series has been expanded. By choosing a few more such points, the several Taylor Series can be blended to produce the entire LCO response with sufficient accuracy.

IV. Transonic Flutter and LCO of Lifting Surfaces

This section* begins with a discussion of generic nonlinear aeroelastic behavior of wings especially as it relates to Limit Cycle Oscillations (LCO); then the important studies that come from flight experience with LCO are noted which have stimulated much of the other research on the subject. Next a summary is provided of the primary physical sources of fluid and structural nonlinearities that can lead to nonlinear aeroelastic response in general and LCO more particularly.

* This section is an abbreviated and revised version of [1].

A brief summary of unsteady aerodynamic models, both linear and nonlinear, is then given before turning to the heart of the section that provides a critique of the results obtained to date via various methods using as a framework correlations between theory and experiment.

A. Generic Nonlinear Aeroelastic Behavior

There are several basic concepts that will be helpful for the reader to keep in mind throughout the discussion to follow. The first is the distinction between a static nonlinearity and a dynamic one. In the aeroelasticity literature the term "linear system" may either mean a (mathematical or wind tunnel) model or flight vehicle that is both statically and dynamically linear in its response or one that is nonlinear in its static response, but linear in its dynamic response. So we will usually qualify the term "linear model" further by noting whether the system is dynamically linear or both statically and dynamically, i.e. wholly linear.

An example of a system which is wholly linear is a structure whose deformation in response to either static or dynamic forces is (linearly) proportional to those forces. An aerodynamic flow is wholly linear when the response (say change in pressure) is (linearly) proportional to changes in downwash or fluid velocities induced by the shape or motion of a solid body in the flow. This is the domain of classical small perturbation aerodynamic theory and leads to a linear mathematical model (convected wave equation) for the fluid pressure perturbation or velocity potential. Shock waves and separated flow are excluded from such flow models that are both statically and dynamically linear. A wholly linear aeroelastic model is of course one composed of wholly linear structural and aerodynamic models.

A statically nonlinear, but dynamically linear structure is one where the static deformations are sufficiently large that the static response is no longer proportional to the static forces and the responses to the static and dynamic forces cannot simply be added to give meaningful results. Buckled skin panels (buckling is a nonlinear static equilibrium that arises from a static instability) that dynamically respond to (not too large) acoustic loads or the prediction of the onset of their dynamic aeroelastic instability (flutter) are examples where a statically nonlinear, but dynamically linear model may be useful.

In aerodynamic flows, shock waves and separated flows are themselves the result of a dynamically nonlinear process. But once formed they may often be treated in the aeroelastic context as part of a nonlinear static equilibrium state (steady flow). Then the question of the dynamic stability of the statically nonlinear fluid-structural (aeroelastic) system may be addressed by a linear dynamic perturbation analysis about this nonlinear static equilibrium. Sometime such aerodynamic flow models are call time linearized.

Of course if one wishes to model limit cycle oscillations and the growth of their amplitude as flow parameters are changed, then either or both the structural and the aerodynamic model must be treated as dynamically nonlinear. Often a single nonlinear mechanism is primarily responsible for the limit cycle oscillation. However, one may not know apriori which nonlinearity is dominant unless one has designed a mathematical model, wind tunnel model or flight vehicle with the chosen nonlinearity. Not the least reason why limit cycle oscillations are more difficult to understand in flight vehicles (compared to say mathematical models) is that rarely has a nonlinearity been chosen and designed into the vehicle. More often one is dealing with an unanticipated and possibly unwanted nonlinearity. Yet sometimes that nonlinearity is welcome because without it the limit cycle oscillation would instead be replaced by catastrophic flutter leading to loss of the flight vehicle.

It must be emphasized that the variety of possible nonlinear aeroelastic responses is not limited to 'Limit Cycle Oscillations (LCO)' per se. In the context of nonlinear system theory [41], an LCO is one of the simplest dynamic bifurcations. Other common possible nonlinear responses include higher harmonic and subharmonic resonances, jump-resonances, entrainment, beating and period doubling to name only a few. These responses have been studied using low order model problems in the nonlinear dynamics literature; however in aeroelastic wind tunnel and flight testing the detailed knowledge required to identify these nonlinear responses has rarely been available.

Now consider the generic types of nonlinear dynamic response that may occur, i.e. limit cycle oscillations and the variation of their amplitude with flight speed (or wind tunnel velocity). Of course the frequency of the LCO may vary with flight parameters as well, but usually the frequency is near that predicted by a classical linear dynamic stability (flutter) analysis.

The generic possibilities are indicated in Figure 11a and 11b where the limit cycle amplitude is plotted vs. some system parameter, e.g. flight speed. In Figure 11a, an aeroelastic system is depicted that is stable to small or large disturbances (perturbations) below the flutter (instability) boundary predicted by a linear dynamical model. Beyond the flutter boundary, LCO arise due to some nonlinear effect and typically the amplitude of the LCO increases as the flight speed increases beyond the flutter speed. In Figure 11b, the other generic possibility is shown. While again LCO exist beyond the flutter boundary, now LCO may also exist below the flutter boundary, if the disturbances to the system are sufficiently large. Moreover both stable (solid line) and unstable (dotted line) LCO now are present.

Stable LCO exist when for any sufficiently small disturbance, the motion returns to the same LCO at large time. Unstable LCO are those for which any small perturbation will cause the motion to move away from the unstable LCO and move toward a stable LCO. Theoretically, in the absence of any disturbance both stable and unstable LCO are possible dynamic, steady state motions of the system. Information about the size of the disturbance required to move from one stable LCO to another can also be obtained from data such as shown in Figure 11b. Note also the hysteretic response as flight speed increases and then decreases.

B. Flight Experience with Nonlinear Aeroelastic Effects

Much of the flight experience with aircraft LCO has been documented by the Air Force SEEK EAGLE Office at Eglin AFB and is described in several publications by Denegri and his colleagues [42-45]. Most of this work has been in the context of the F-16 aircraft. Denegri distinguishes among three types of LCO based upon the phenomenological observations in flight and as informed by classical linear flutter analysis. "Typical LCO" is when the LCO begins at a certain flight condition and then with say an increase in Mach number at constant altitude the LCO response smoothly increases. "Flutter", as distinct from LCO, is said to occur when the increase in LCO amplitude with change in Mach number is so rapid that the safety of the vehicle is in question. And finally "atypical LCO" is said to occur when the LCO amplitude first increases and then decreases and perhaps disappears with changes in Mach number. This is also sometimes called a "hump" mode. Often changes in flight vehicle angle of attack lead to similar generic LCO responses to those observed with changes in Mach number.

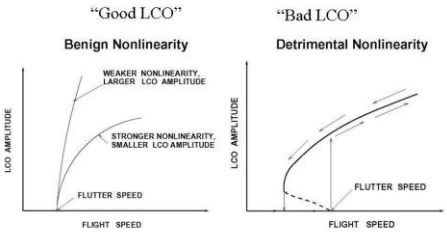

Schematic of Limit Cycle Oscillation Response

Figures 11a and 11b

It has long been recognized [46] that the addition of external stores to aircraft changes the dynamic characteristics and may adversely affect flutter boundaries. Limit cycle oscillations (LCO) remain a persistent problem on high performance fighter aircraft with multiple store configurations. Using measurements obtained from flight tests, Bunton and Denegri [47] describe LCO characteristics of the F-16 and F/A-18 aircraft. While LCO can be present in any sort of nonlinear system, in the context of aeroelasticity, LCO typically is exhibited as an oscillatory response of the wing, the amplitude of which is limited, but dependent on the nature of the nonlinearity as well as flight conditions, such as speed, altitude, and Mach number. The LCO motion is often dominated by antisymmetric modes. LCO are not described by standard linear aeroelastic analysis, and they may occur at flight conditions below those at which linear instabilities such as flutter are predicted. Although the amplitude of the LCO may rise above structural failure limits, more typically the presence of LCOs results in a reduction in vehicle performance, leads to airframe-limiting structural fatigue, and compromises the ability of pilots to perform critical mission-related tasks. When LCO are unacceptable, extensive and costly flight tests for aircraft/store certification are required.

Denegri [42,43] suggests that for the F-16, the frequencies of LCO might be identified by linear flutter analysis; however, linear analysis fails to predict the oscillation amplitude or the onset velocity for LCO. Thus, nonlinear analysis will be necessary to predict the onset of the LCO and their amplitudes with changing flight conditions.

1. Nonlinear Aerodynamic Effects

There are several other flight experiences with limit cycle oscillations in addition to the F-16 including those for example with the F-18, the B-1 and B-2. Most of these LCO have been attributed by investigators to nonlinear aerodynamic effects due to shock wave motion and/or separated flow. However, there is the possibility that nonlinear structural effects involving stiffness, damping or freeplay may play a role as well. Indeed, much of the present day research and development effort is devoted to clarifying the basic mechanisms responsible for nonlinear flutter and LCO. For an authoritative discussion of these issues see Cunningham et al [48-50], Denegri [41-45] on the F-16 and F-18, Dobbs [51], Hartwich [52] on the B-1 and Britt, Jacobsen and Dreim [53] on the B-2. Recent experimental evidence from wind tunnel tests is beginning to shed further light on these matters as are advances in mathematical and computational modeling.

2. Freeplay

There have been any number of aircraft that have experienced flutter induced limit cycle oscillations as a result of control surface freeplay. These are not well documented in the public literature, but are more known by word of mouth among practitioners and perhaps documented in internal company reports and/or restricted government files.

A recent and notable exception is the account in Aviation Week and Space Technology by Croft [54] of a flutter/limit cycle oscillation as a result of freeplay. In many ways this account is typical. The oscillation is of limited amplitude and there was a reported disagreement between the manufacturer and the regulating governmental

agency as to whether this oscillation was or was not sufficiently large as to be a threat to the structural integrity of the aircraft structure. See also Section 3.2 of this paper.

3. Geometric Structural Nonlinearities

Another not infrequently encountered and documented case is the limit cycle oscillation that follows the onset of flutter in plate-like structures. The structure has a nonlinear stiffening as a result of the tension induced by mid-plane stretching of the plate that arises from its lateral bending. This is most commonly encountered in what is often called panel flutter where a local element of a wing or fuselage skin encounters flutter and then a limit cycle oscillation. There have been many incidents reported in the literature dating back to the V-2 rocket of World War II, the X-15, the Saturn Launch Vehicle of the Apollo program and continuing on to the present day. Some of these are discussed in a monograph by Dowell [55] and also a NASA Special Publication by Dowell [56]. See also Section 3.1 of this paper.

It has been recently recognized that low aspect ratio wings may behave as structural plates and thus the entire wing may undergo a form of plate-like flutter and limit cycle oscillations. This has been seen in both wind tunnel models and computations to be discussed later. However there is not yet a clearly documented case of such behavior in flight.

C. Physical Sources of Nonlinearities

Several physical sources of nonlinearities have been identified through mathematical models (in almost all cases), wind tunnel tests (in several cases) and flight tests (less often). Among those most commonly studied and thought to be important are the following. Large shock motions may lead to a nonlinear relationship between the motion of the structure and the resulting aerodynamic pressures and forces that act on the structure. If the flow is separated (perhaps in part induced by the shock motion) this may also create a nonlinear relationship between structural motion and the consequent aerodynamic flow field.

Structural nonlinearities can also be important and are the result of a given (aerodynamic) force on the structure creating a response that is no longer (linearly) proportional to the applied force. Freeplay and geometric nonlinearities are prime examples (already mentioned). But the internal damping forces in a structure may also have a nonlinear relationship to structural motion, with dry friction being an example that has received limited attention to date. Because the structural damping is usually represented empirically even within the framework of linear aeroelastic mathematical models, not much is known about the fundamental mechanisms of damping and their impact on flutter and LCO.

All of these nonlinear mechanisms have nevertheless been considered by the mathematical modeling community and several have been the subject of wind tunnel tests as well. In some cases good correlation between theory and experiment has been obtained for limit cycle oscillation response.

D. Efficient and Accurate Computation of Unsteady Aerodynamic Forces: Linear and Nonlinear

The literature on unsteady aerodynamic forces alone is quite extensive. A comprehensive assessment of current practice in industry is given by Yurkovich, Liu and Chen [57]. An article that focuses on recent developments is that of Dowell and Hall [3]. Other recent and notable discussions include those of Bennett and Edwards [58] and Lucia, Beran and Silva [4]. Much of the present focus of work on unsteady aerodynamics is on developing accurate and efficient computational models. Standard computational fluid dynamic [CFD] models and solution methods that include the relevant fluid nonlinearities are simply too expensive now and for some time to come for most aeroelastic analyses. Thus there has been much interest in reducing computational costs while retaining the essence of the nonlinear flow phenomena. See Section 3.3 of this paper.

E. Experimental/Theoretical Correlations

Much of what we know about the state of the art with respect to nonlinear aeroelasticity comes from the study of correlations between experiment and theory and between various levels of theoretical models. Hence the remainder of this discussion is largely devoted to such correlations and the lessons learned from them. The correlations selected are representative of the state of the art for transonic flutter boundaries and limit cycle oscillations.

Flutter Boundaries in Transonic Flow:

AGARD 445.6 WING MODELS – Bennett and Edwards [58] have discussed the state of the art of Computational Aeroelasticity (CAE) in a relatively recent paper and made several insightful comments about various correlation studies. The NASA Langley team pioneered in providing correlations for the AGARD 445.6 wing in the transonic flow region. For this thin wing, there are no significant transonic effects in the steady flow over the wing surface at

the Mach numbers with experimental results except for M=0.96 where there is a very weak shock on the surface. For the subsonic conditions, all computational results are in very good agreement with experiment. However, the two low supersonic test conditions have been problematic for CAE. Inviscid flow (Euler) computations have produced high flutter speed index (FSI) values relative to the experimental FSI and viscous flow (Navier-Stokes) computations have accounted for about one half the difference between theory and experiment. Several investigators have now done similar Euler calculations and obtained similar results [59-61]. The excellent agreement of the wholly linear theory results with experiment should probably be regarded as fortuitous. Interestingly, Gupta [62], who also used an Euler based CFD model, obtains results in better agreement with experiment at the low supersonic conditions, though in less good agreement with experiment than the other Euler based results at subsonic conditions. Thus, CAE computations for this low supersonic region have unresolved issues which probably involve details such as wind tunnel wall interference effects and flutter test procedures, as well as CAE modeling issues.

HSCT Rigid and Flexible Semispan Models – Two semispan models representative of High Speed Civil Transport (HSCT) configurations were tested in the NASA Langley Research Center Transonic Dynamics Tunnel (TDT) in heavy gas. A Rigid Semispan Model (RSM) was tested mounted on an Oscillating Turn Table (OTT) and on a Pitch And Plunge Apparatus (PAPA). The RSM/OTT test [63] acquired unsteady pressure data due to pitching oscillations and the RSM/PAPA test acquired flutter boundary data for simple pitching and plunging motions. The RSM test [64] involved an aeroelastically-scaled model and was mounted to the TDT sidewall. The test acquired unsteady pressure data and flutter boundary data. The results show the unexpectedly large effect of mean angle of attack upon the flutter boundaries for the RSM/PAPA model. Flutter of thin wings at subsonic conditions is typically independent of angle-of-attack within the linear flow region. A region of increased response in first wing bending (8.5 Hz.) was encountered in the Mach number range of 0.90-0.98. Finally, a narrow region of LCO behavior, labeled 'chimney', was encountered for M = 0.98-1.00 and over a wide range of dynamic pressures.

Benchmark Active Control Technology (BACT) Model - This rectangular wing model had an aspect ratio of two and a NACA 0012 airfoil section. [65,66] It was mounted on a pitching and plunging apparatus which allowed flutter testing with two structural degrees of freedom. It was extensively instrumented with unsteady pressure sensors and accelerometers and it could be held fixed (static) for forced oscillation testing or free for dynamic response measurements. Data sets for trailing-edge control surface oscillations and upper-surface spoiler oscillations for a range of Mach numbers, angle of attack, α, and static control deflections are available. The model exhibited three types of flutter instability.

A classical flutter boundary was found for $\alpha = 2$ deg, as a conventional boundary of flow density versus Mach number with a minimum, the transonic 'dip', near M = 0.77 and a subsequent rise. Stall flutter was found, for $\alpha > 4$ deg, near the minimum of the flutter boundary (and at most tunnel conditions where high angles of attack could be attained). Finally, a narrow region of instability occurred near M = 0.92 consisting of plunging motion at the plunge mode wind-off frequency. This type of transonic instability has sometimes been termed single-degree-of-freedom flutter. It is caused by the fore and aft motion of symmetric shocks on the upper and lower surfaces for this wing. It was very sensitive to any biases and did not occur with nonzero control surface bias or nonzero alpha. Such a stability boundary feature is sometimes termed a 'chimney' since the oscillations are typically slowly diverging or constant amplitude (LCO) and it is found, sometimes, that safe conditions can be attained with small further increases in Mach number.

Computational studies by Kholodar et al [67] were conducted to correlate with the flutter boundary obtained experimentally by Rivera et al [68]. Kholodar's inviscid calculation agreed very well with the experimental findings except for $M \approx 0.88$ to $M \approx 0.95$ where a "plunge instability region" occurred.

Experimental data for the flutter boundary were not obtained at Mach numbers just below the plunge instability region. Using an inviscid aerodynamic model in the flutter calculations, no flutter solutions could be obtained for $0.82 < M < 0.92$ except at very low flow densities (inverse mass ratios). This is approximately the same region for which experimental results were unavailable. Kholodar conjectured this indicated that in this region, the flutter mass ratio (inversely proportional to flow density or dynamic pressure) rose precipitously as the airfoil entered a single degree-of-freedom flutter mode. Conversely, flow density (or inverse mass ratio) dropped precipitously.

Viscous CFD results obtained by Schwarz et al [69] revealed a number of surprising characteristics. First, whereas inviscid aerodynamics made flutter solutions difficult to find in the region $0.82 \le M \le 0.91$ due to the sharp increase in flutter mass ratio, μ; by contrast, viscous results on a 193 x 49 CFD grid yielded readily detectable solutions. However, these viscous solutions showed some sensitivity to Mach number.

A grid refinement study was performed by Schwarz et al [69] to verify the results obtained on the nominal 193 x 49 grid. The flutter condition was recomputed on a coarser 97 x 25 grid and also a fine 385 x 97 grid at select Mach numbers, chosen to be representative of the range of Mach numbers examined. This study showed that the coarse 97 x 25 grid had insufficient resolution and produced results in poor agreement with experiment at low subsonic as well as transonic Mach numbers.

Results on the 385 x 97 computational mesh agreed with those on the nominal 193 x 49 mesh except for a narrow range of transonic Mach numbers. For $M \approx 0.84 - 0.86$, computations on this mesh showed flow shedding to be occurring, a phenomenon not seen on the coarser meshes (shedding or buffeting is an LCO of the flow alone, even in the absence of structural motion). The range in which this shedding occurred agrees very closely with the Mach number range for which experimental results were not obtained, approximately $0.82 < M < 0.88$. As seen in Figure 12, predictions on the 193 x 49 and 385 x 97 viscous grids largely agreed outside of this shedding region.

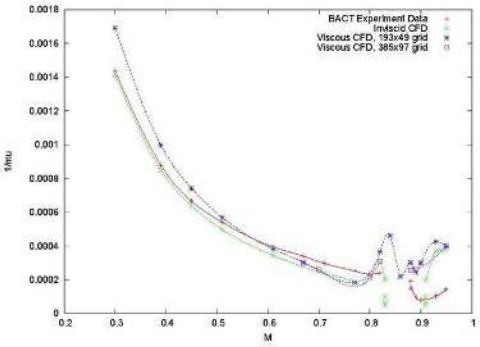

Figure 12: Flutter inverse mass ratio versus Mach number from viscous and inviscid CFD results and experimental data from Rivera [68].

Shedding or buffeting prohibits a linear flutter analysis at the Mach numbers for which it occurs, because it violates the assumption that the flow behaves in a dynamically linear way for small motions of the airfoil. Still, the present calculation provides an insight into the flutter experiment. The occurrence of shedding correlates with the range of Mach numbers for which airfoil motions became erratic in the experiments, indicating that shedding may have led to this unusual behavior.

F-16

The computed flutter boundaries for eight F-16 wing/store configurations are shown in Figure 13 in terms of altitude versus Mach number based upon standard atmospheric conditions. Note the Mach number range over which flutter may occur varies substantially from one configuration to the next. In these calculations, the viscous Reynolds Averaged Navier Stokes (RANS) version of the Duke University harmonic balance solver was used [70]. Calculations for some of these configurations were also done using an Euler version of the CFD code. In general, the Euler code provides similar trends for the flutter onset boundary, but there are some quantitative differences, i.e. as much as 25%.

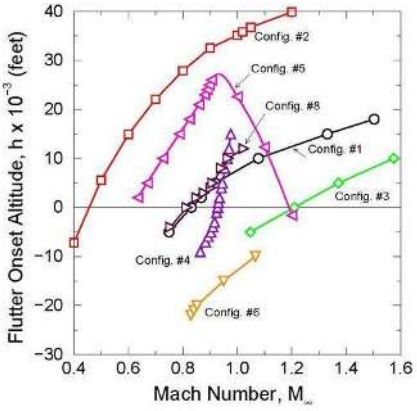

Figure 13: Computed F-16 Fighter Flutter Onset Altitude versus Mach Number

Note that in Figure 13 there are no results for Configuration #7. This is because no flutter or LCO was found in the Mach number range shown which is in agreement with the flight test results. Also for configuration #6, flight tests were stopped at Mach numbers less than the highest shown in Figure 13. Again no flutter or LCO was found in the flight test in agreement with the computations. Moreover the computed flutter boundaries shown in Figure 13 generally agree reasonably well with the flight test results as seen in Figure 14. Note that a range of Mach number is shown for configuration #5 for both computed and flight test results in Figure 14. This is because flutter and LCO occur over a range of Mach number for configuration #5 with flutter/LCO starting at the lowest Mach number shown and ending at the highest Mach number shown. Recall Figure 13. This is sometimes called a "hump" flutter/LCO mode.

A comparison between measured and computed frequencies at Mach numbers just beyond the onset of LCO for the several configurations where LCO was observed shows the agreement is generally quite good and it is noted that the LCO frequency does not vary rapidly with Mach number [70].

Limit Cycle Oscillations:

- **Airfoils with structural stiffness and freeplay nonlinearities**

Some investigators have considered configurations with a variety of nonlinear stiffness and freeplay structural nonlinearities. For a description of the work on freeplay nonlinearities, see the article by Dowell and Tang [71] which focuses on correlations between theory and experiment as well as Section 3.2 of the present paper. In general good quantitative correlation is found for simple wind tunnel models and the basic physical mechanism that leads to LCO appears well understood. Among the important insights developed include the demonstration that the LCO amplitude and the effect of mean angle of attack on LCO amplitude both simply scale in proportion to the range of freeplay present in the aeroelastic system. This result has received further confirmation from the excellent study of Schlomach for the F-35 aircraft program [18].

An example of another stiffness nonlinearity is described next.

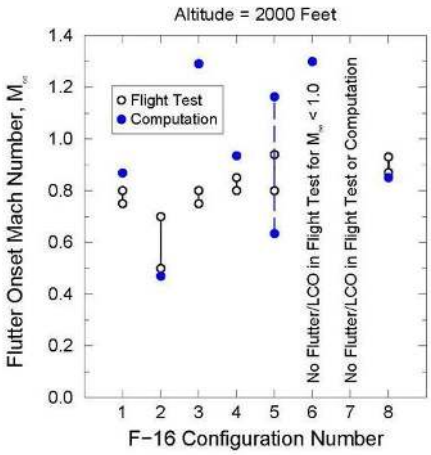

Figure 14: Flutter Mach Number Characteristics for Each F-16 Fighter Configuration

- **Delta wings with geometrical plate nonlinearities**

At low Mach numbers good correlation has been demonstrated between theory and experiment for LCO amplitudes and frequencies. Since these results are well documented elsewhere, see Dowell and Tang [71], here the recent work of Gordnier et al [72,73] that has extended these correlations into the transonic range for a cropped delta wing planform is emphasized. This configuration had been investigated experimentally by Schairer and Hand [74] and the theoretical calculations were done by Gordnier et al using both Euler and Navier-Stokes flow models. Initially the theoretical calculations were done using a linear structural model, which gave predicted LCO amplitudes much greater than those observed experimentally. This led Gordnier to include nonlinearities in the structural model via Von Karman's nonlinear plate theory that provided much improved correlation between theory and experiment. Note that the effects of viscosity are modest based upon the good agreement of results using the Euler vs Navier-Stokes models. Also the much improved agreement obtained with the nonlinear structural model suggests that aerodynamic nonlinearities per se are not as significant for this configuration as are the structural nonlinearities.

- **Large shock motions and flow separation**

These aerodynamic nonlinearities are both the most difficult to model theoretically and also to investigate experimentally. Hence it is not surprising that our correlations between theory and experiment are not yet what we might like them to be. As a corollary one might observe that it will in all likelihood be easier to design a favorable nonlinear structural element to produce a benign LCO, than to assure that flow nonlinearities will always be beneficial with respect to LCO.

AGARD 445.6 Wing Models

The AGARD 445.6 wing has been discussed earlier in terms of its flutter boundary; now we turn to results from Thomas, Dowell and Hall [75] for LCO. The correlation between theory and experiment for the flutter boundary is shown in Figure 15 where the Euler flow model is that of Thomas et al. But now we have in addition results for LCO amplitude versus FSI for various Mach number. See Figure 16. Note that a value of first mode non-dimensional modal amplitude of ξ=0.012 as shown in this figure corresponds to a wing tip deflection equal to one fourth of the wing half-span. Note there is no Mach number for which a benign LCO is predicted and subcritical LCO is predicted at M=1.141 and 1.072. This means that LCO may occur below the flutter boundary at these two Mach numbers and perhaps this explains at least in part why flutter (or really an unstable LCO) occurred in the experiment below the predicted flutter boundary.

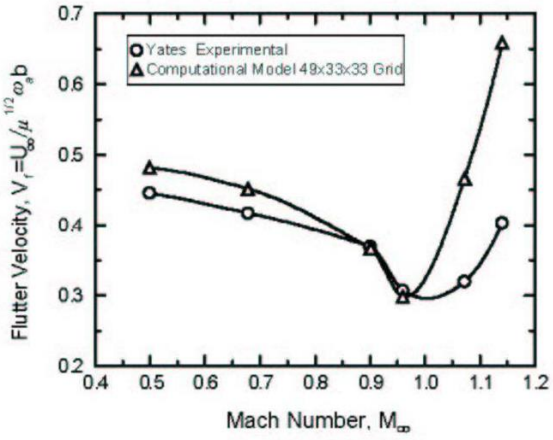

Figure 15: Flutter Speed Index vs. Mach Number for AGARD Wing 445.6: Comparison of Theory and Experiment

Small amplitude LCO behavior for the AGARD 445.6 wing has also been calculated by Edwards [76]. The majority of published calculations for this wing model (actually a series of models with similar planforms) are for the "weakened model #3" tested in air, since this test covered the largest transonic Mach number range and showed a significant transonic dip in the flutter boundary. The focus on this particular configuration may be in some ways unfortunate, in that the model tested in air resulted in unrealistically large mass ratios and small reduced frequencies. Weakened models #5 and #6 were tested in heavy gas and had smaller mass ratios and higher reduced frequencies. Very good agreement was obtained with experiment for flutter speed index using the CAP-TSDV code over the Mach number range tested. For the highest Mach number tested, M=0.96, it was noted that damping levels extracted from the computed transients were amplitude dependent, an indicator of nonlinear behavior. It was also found that small amplitude divergent (in time) responses used to infer the flutter boundary would transition to LCO when the calculation was continued further in time. The wing tip amplitude of the LCO was approximately 0.12 inches peak-to-peak, a level that is unlikely to be detected in wind tunnel tests given the levels of model response to normal wind tunnel turbulence.

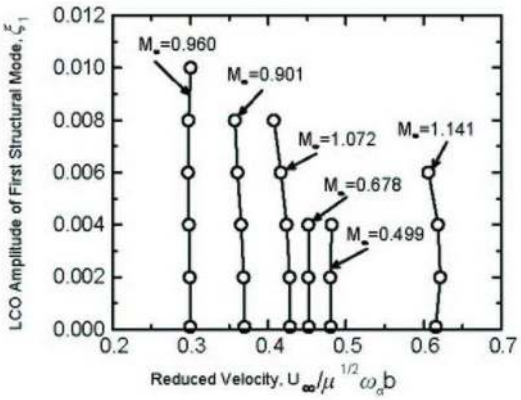

Figure 16: LCO Amplitude vs Flutter Speed Index (Reduced Velocity) for Various Mach Number for AGARD 445.6 Wing

MAVRIC Wing Flutter Model – This business jet wing-fuselage model (see Edwards [77,78]) was chosen by NASA Langley Research Center's Models For Aeroelastic Validation Involving Computation (MAVRIC) project with the goal of obtaining experimental wind-tunnel data suitable for Computational Aeroelasticity (CAE) code validation at transonic separation onset conditions. LCO behavior was a primary target. An inexpensive construction method of stepped-thickness aluminum plate covered with end-grain balsa wood and contoured to the desired wing profile was used. A significant benefit of this method was the additional strength of the plate that enabled the model to withstand large amplitude LCO motions without damage.

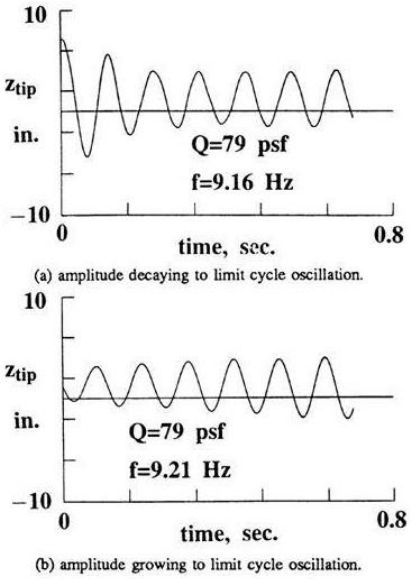

Figure 17: Transient Response Leading to a LCO: Simulation for Mavric Wing

The behavior of the MAVRIC model as flutter was approached during the wind tunnel test indicated that wing motions tended to settle to a large amplitude LCO condition, especially in the Mach number range near the minimum FSI conditions. Figure 17 demonstrates [78] the ability of the CAP-TSDV code to simulate these large amplitude LCO motions. Large and small initial condition disturbance transient responses clearly show the six inch peak-to-peak wingtip motions observed in the tests. Such large amplitude aeroelastic motions have not been demonstrated by RANS CFD codes which have difficulty maintaining grid cell structure for significant grid deformations. Figure 18 shows the map of the regions of LCO found in the MAVRIC test in the vicinity of the minimum FSI (clean wingtip, $\alpha = 6$ deg.) [78]. Numbers for the several contours in the figure give the half-amplitude of wingtip LCO motions, in g's, in the indicated regions. Two regions, signified by 'B', are regions where 'beating' vibrations were observed. For this test condition, wing motions are predominantly of the wing first bending mode at a frequency of 7-8 Hz. (wind-off modal frequency is 4.07 Hz.). Two chimney features are seen, at M ~ 0.91 and at M ~ 0.94. Edwards discusses flutter model responses which are indicative of more complex nonlinear behaviors than are commonly attributed to LCO. Thus, flutter test engineers are familiar with responses such as 'bursting' and 'beating,' commonly used as indicators of the approach to flutter (and LCO).

Clipped-Tip Delta Wing Control Surface Buzz Model – Parker et al [79] describe a test of a clipped-tip delta wing model with a full span control surface. The tests were conducted in air which is of concern since there are known to be severe Reynolds number and/or transition effects for this tunnel at dynamic pressures below 50-75 pounds per square foot. Pak and Baker [80] have performed computational studies of this case. They compare the experimental buzz boundary with time-marching transient responses calculated with the CFL3D-NS code and the CAP-TSDV code, respectively. Both codes capture LCO behavior near the experimental buzz conditions with the higher level code appearing to have better agreement for the experimental trend versus Mach number. The record lengths of a number of the responses, which are extremely expensive to compute, are not sufficient for clear determination of the response final status. Also, LCO behaviors can result from very delicate force balances and settling times to final LCO states can require many cycles of oscillation.

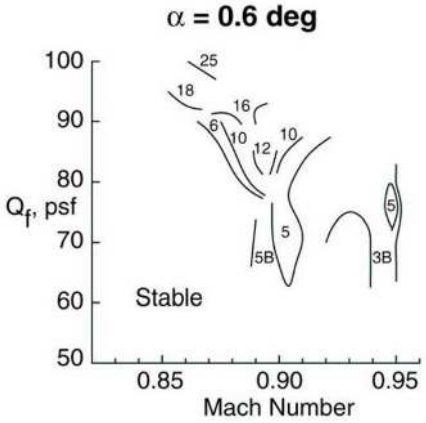

Figure 18: Dynamic Pressure vs. Mach Number Contours of Constant LCO Amplitude for Mavric Wing

Residual Pitch Oscillations on the B-2 – The B-2 bomber encountered a nonlinear aeroelastic Residual Pitch Oscillation (RPO) during low altitude high speed flight [53]. Neither the RPO nor any tendency of lightly damped response had been predicted by wholly linear aeroelastic design methods. The RPO involved symmetric wing bending modes and rigid body degrees of freedom. It was possible to augment the CAP-TSDV aeroelastic analysis code with capability for the longitudinal short-period rigid body motions, vehicle trim, and the full-time active flight control system including actuator dynamics. This computational capability enabled the analysis of the heavyweight, forward center of gravity flight condition [53]. The simulation predicts open loop instability at M = 0.775 and closed loop instability at M = 0.81 in agreement with flight test. In order to capture the limit cycle behavior of the RPO it was necessary to include modeling of the nonlinear hysteretic response characteristic of the B-2 control surfaces for small amplitude motions. This is caused by the small overlap of the servohydraulic control valve spool flanges with their mating hydraulic fluid orifices. With this realistic actuator modeling also included, limited amplitude RPO motions similar to those measured in flight were simulated. A lighter weight flight test configuration exhibited very light damping near M = 0.82 but did not exhibit fully developed RPO. Instead damping increased with slight further increase in speed, typical of hump mode behavior. The CAP-TSDV simulations did not capture this hump mode behavior.

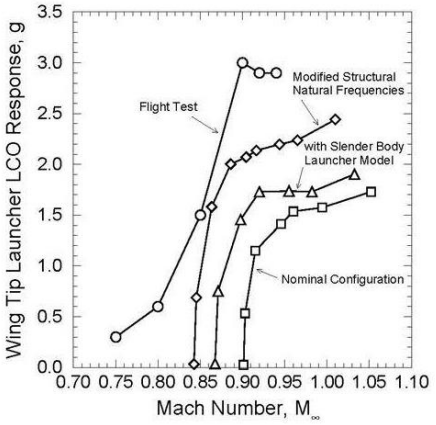

Figure 19: F-16 Configuration #1 Computed and Flight Test Forward Wingtip Launcher Accelerometer LCO Response Level versus Mach Number for an Altitude of 2000 feet and a Mean Angle-of-Attack *of* α_0=1.5 degrees.

F-16 – In Figure 19, a comparison of computational and flight test results is shown for Configuration #1 for both the flutter boundary and also for LCO response [70]. This is a plot of wing tip acceleration response versus Mach number at a fixed altitude of 2000 feet. The flight test results are shown by the curve with open circles. Three different computational results are shown. The curve with open squares shows the results for the nominal configuration with the aerodynamics of the stores neglected. The curve with open triangles includes the effects of the aerodynamics of the wing tip launcher using slender body aerodynamic theory. Note this curve is in better agreement with the flight test data. Finally the curve with open diamonds is for a one percent change in one of the structural frequencies. Here the computational model has been "tuned" to the experiment to give better agreement with the measured LCO frequency. That in turn has led to better agreement between computation and measurement for the LCO amplitude. Of course if a change in structural frequency in the opposite direction is made, this leads to poorer agreement between computations and flight test with the LCO response curve moving a similar amount from the nominal response but in the opposite direction. So what has been shown by the "tuning" is that the results for this configuration are sensitive to small plausible changes in the structural frequencies.

A final word about the correlation between computations and flight test is warranted. Note that the computations show a precise Mach number at which flutter and the onset of LCO occurs, i.e. when the wing tip acceleration is zero. This is because we have neglected the gust response of the aircraft to atmospheric turbulence as is traditional in flutter and LCO calculations. Of course in the flight test there is always some (small) response even when there is no flutter or LCO due to atmospheric turbulence. Thus it is impossible to define a precise Mach number at which flutter begins from the flight test data shown in Figure 19. Indeed inferring a flutter Mach number from flight test data is a difficult art and requires a deeper study of the test data than simply a plot such as shown in Figure 19. On the other hand, for the present purpose, this is not crucial. From Figure 19, it is clear that neither flutter nor LCO is occurring for Mach numbers less than M_∞= 0.8, but flutter onset and LCO do occur for Mach numbers greats than M_∞= 0.85. And thus one can compare the computed flutter Mach number to this range from the test data. For LCO per se, the major goals are predicting the maximum LCO response level and the frequency and structural modal content of the LCO. The frequency and modal content are well predicted by the computational model [70], and the maximum response is reasonably well predicted as well for this configuration. See Figure 19. Note in particular that both flight test and computations show the flutter and LCO motion is anti-symmetric.

Time Marching Codes Compared to Various Experimental Results - In the paper by Huttsell et al [81] several state of the art time marching CFD codes are used to investigate flutter and LCO for challenging cases drawn from flight or wind tunnel tests. The CAP-TSD, CAP-TSDV, CFL3D and ENS3DAE codes are all used. The results are extremely helpful in providing a realistic assessment of the state of the art of these codes and they are also indicative future needs and improvements. For the F-15 aircraft example, difficulty was encountered in producing a computational grid with negative volumes being encountered. For the AV8-B aircraft a steady state flow field could not be found due to oscillations in the numerical solver from one iteration to the next. These difficulties are not unusual for CFD codes in the present authors' experience. Sometimes the difficulty in achieving a steady flow solution is attributed to shedding in the flow field, but in the absence of a full nonlinear dynamic CFD calculation, that must remain a speculation. For the B-2 aircraft example encouraging agreement was obtained for the frequency and damping variation of the critical flutter (and LCO) mode as a function of flight speed using the CAP-TSDV code. For the B-1 estimates of the damping associated with LCO were computed using the CFL3DAE code and favorably compared to those found in wind tunnel tests. It is not entirely clear what the "damping" of an LCO means, however, since by definition LCO is a neutrally stable motion. Two control surface "buzz" cases were considered and CFL3DAE had some success in predicting the behavior observed in the wind tunnel for a NASP like configuration.

As Huttsell et al [81] note, additional work is needed to improve CFD model robustness, computational efficiency and grid deformation strategies.

V. Aerodynamic LCO: Buffet, AWS and NSV

The aerodynamic flow field itself can become unstable even in the absence of any structural motion. Of course, once the flow field becomes unstable, then oscillations in the flow will begin and due to aerodynamic nonlinearities such as shock motion and/flow separation a limit cycle oscillation may (and usually will) occur. This purely aerodynamically generated LCO may then drive the structure into motion and the structural motion may in turn modify the LCO. Often in practice it is difficult to distinguish this type of LCO from one that occurs because of an inherent aeroelastically generated LCO in which the aerodynamic flow per se is stable. Of course in mathematical models this distinction can be (but is not always) made clear. But in a wind tunnel or flight test it is more difficult to distinguish between these two different LCO scenarios.

Even so, in recent years considerable progress has been made in understanding aerodynamically generated LCO and subsequent aeroelastic effects. This progress is briefly summarized here and the promise of greater progress in the future is substantial.

In classical aerodynamics the transition from laminar to turbulent flow is one of the most important examples of a steady (laminar) fluid flow becoming unstable and thus leading to a (turbulent) fluid flow LCO. Determining the properties of this LCO of turbulence remains one of the great unresolved issues of all of science and engineering.

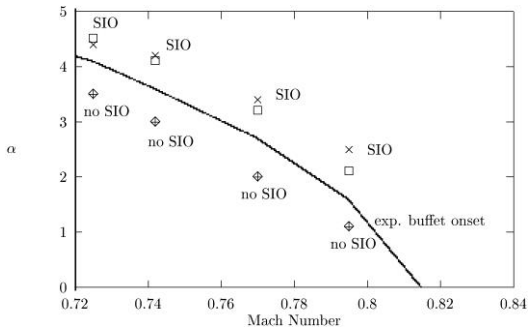

Figure 20: Buffet Boundary: Angle of Attack versus Mach Number

However there are also other examples of flow instabilities which go by such names as buffet, abrupt wing stall (AWS) and non synchronous vibration (NSV), that have received much attention in aerospace (and other) research and engineering applications. Typically, in these examples the flow is already turbulent, but a further dynamic instability occurs whose intensity is far greater than typical turbulence (e.g. the oscillating lift coefficient is of order unity) and whose length scale is of the order of the airfoil or wing dimensions. By contrast, turbulence per se occurs over a great range of length scales including length scales much smaller than a wing chord or span and the intensity is a small fraction of the mean flow values.

Here we discuss the work of Edwards [82], Barakos [83] and Raveh [84-86] on buffet and are content to cite some of the key literature on AWS and NSV.

There is a well known experiment by McDevitt and Okuno [87] that considers the dynamic instability of the flow about a NACA 0012 airfoil in transonic flow conditions at certain prescribed angles of attack. The airfoil itself does not move, but the flow oscillates in what today might be called a limit cycle oscillation (LCO), but is more commonly referred to as a buffeting flow. Several investigators have undertaken computations to compare with these experiments. Edwards [78] has considered a potential flow model for the outer flow coupled to an integral boundary layer model and shown excellent agreement with the measured data for the buffet (LCO) boundary. This boundary is expressed in terms of angle of attack versus Mach number and separates the no buffet (no LCO) region from the buffet (LCO) region. Barakos [79] has also done an interesting study where various turbulence models are used in a Reynolds Averaged Navier-Stokes (RANS) computation and shown that the k-omega and Spalart-Allmaras turbulence models also give good correlation for the buffet (LCO) boundary and the buffet (LCO) frequency. Figure 20 is a comparison of the computed and measured buffet boundary from Barakos [79], who also shows that other commonly used turbulence models such as k-epsilon fail altogether to predict the buffet boundary. Hence buffet experiments [83] and correlations with computational models may give essential and fundamental insights into the required computational fluid dynamics (CFD) models for unsteady aerodynamic flows.

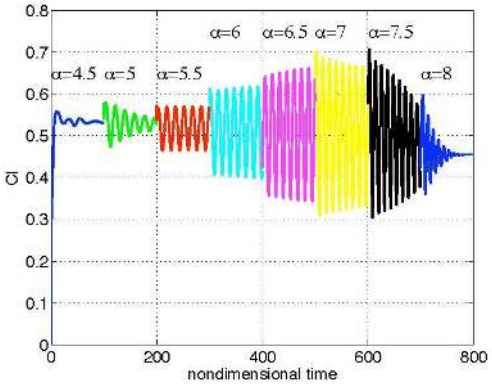

Figure 21a: Lift coefficient vs. time in response to the step-up increments to the mean flow angle of attack; Mach 0.72, Re 1E7.

Very recently Raveh et al [84-86] have studied the effect of a prescribed airfoil motion on a buffeting flow. Many interesting findings have been uncovered including the possibility of "lock-in". Lock-in occurs when response at the inherent flow buffet frequency is suppressed and the flow as well as the airfoil oscillates at the frequency of the prescribed airfoil motion. This occurs for certain combinations of the airfoil motion amplitude and frequency. The larger the airfoil motion, the wider the range of structural frequency (near the buffet flow frequency) for which lock-in will occur. Recently Raveh et al [85] have considered the case of an elastically mounted airfoil which is free to move, but for which there is no prescribed motion. Again lock in is found under certain conditions. It is an open question of how often this may occur in wind tunnel tests or flight tests of aeroelastic systems. However the BACT wind tunnel model discussed earlier [65-69], an elastically mounted rigid wing with a NACA 0012 airfoil profile, is an intriguing example of where such oscillations may have occurred.

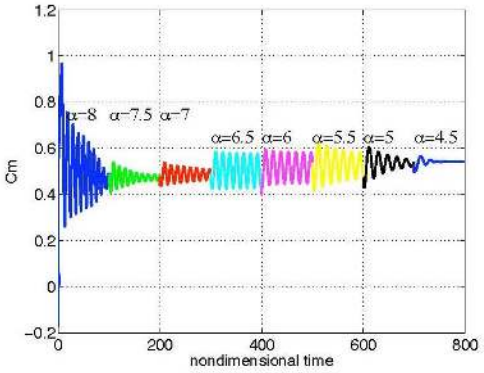

Figure 21b: Lift coefficient vs. time in response to the step-down increments to the mean flow angle of attack; Mach 0.72, Re 1E7

Figure 21 is from [86] and shows the time histories of lift on the NACA 0012 airfoil as the angle of attack is increased in prescribed steps of .5 degrees from 4.5 degrees and then decreased in steps starting from 8.5 degrees. Outside the range of angle of attack for which buffet occurs, a transient decay of the lift illustrates the approach to a time independent steady flow. By contrast, inside the range of angle of attack for which buffet occurs, the long time response is a periodic oscillation of the lift (and other flow variables).

Then a prescribed airfoil motion is added and the effect of this motion on the buffet limit cycle oscillation is found. Figure 22 is also from [86] and shows the lift response on the airfoil for

various cases of prescribed airfoil motion amplitudes and frequencies. This illustrates the approach to lock in when the frequency and amplitude of the prescribed motion are in the appropriate ranges. Figure 23 shows the range for which lock-in occurs in a plot of motion amplitude versus frequency.

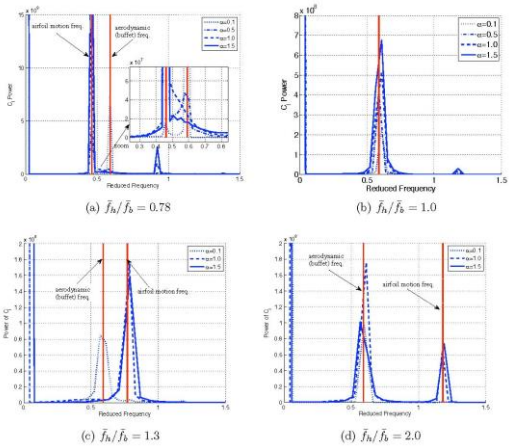

Figure 22: Frequency content of lift coefficient response to prescribed airfoil motion of various amplitudes and frequencies: α_m = 6°, Mach 0.72, Re 1E7.

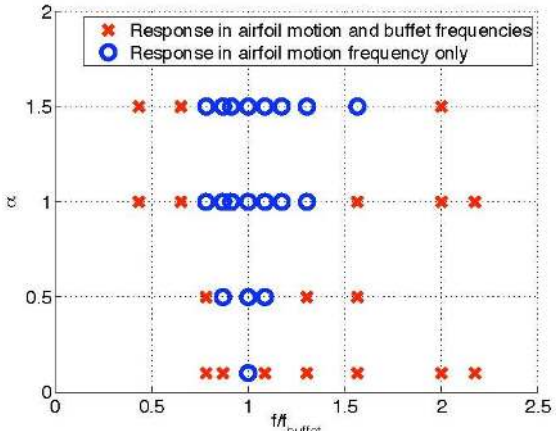

Figure 23: Lock-in map of shock buffet; α_m = 6°, Mach 0.72, Re 1E7

The study of buffeting (and its counterparts of abrupt wing stall and non-synchronous vibration) appears ripe for even more significant advances and also suggests the need for further experiments building on the earlier wind tunnel tests of McDevitt and Okuno and the NASA Langley team with the BACT wind tunnel model. In particular the computational results suggest that one can exit the buffet region by continuing to increase the angle of attack at a given Mach number. Also the computational models are now capable of predicting the buffeting (LCO) amplitudes. Neither of these predictions have yet been validated by experiments, but these important issues could be addressed in new experiments that extend the earlier test results.

Abrupt Wing Stall (AWS) appears to be a particular form of buffet, but with two possible caveats. First of all, the instability of the aircraft flow field appears to be asymmetric and/or anti-symmetric with respect to the fuselage and thus gives rise to an oscillating rolling moment that leads to what is sometimes called "wing drop". At least a dozen distinct aircraft have encountered this phenomenon over several decades, but the ability to predict when it will occur is still beyond current computational modeling methods. Nevertheless there is real hope that this will become possible with a suitable CFD model in the near to mid-term future. Also it is still uncertain to what degree aeroelastic feedback is an issue including the rigid body motions in roll. Much of the recent work on AWS has been done in the context of the F-18 program which devoted very substantial effort to resolving this issue for that aircraft. For a summary and citation to recent literature, see for example [1].

Non-Synchronous Vibration (NSF) appears to be in substantial part a form of buffet encountered in

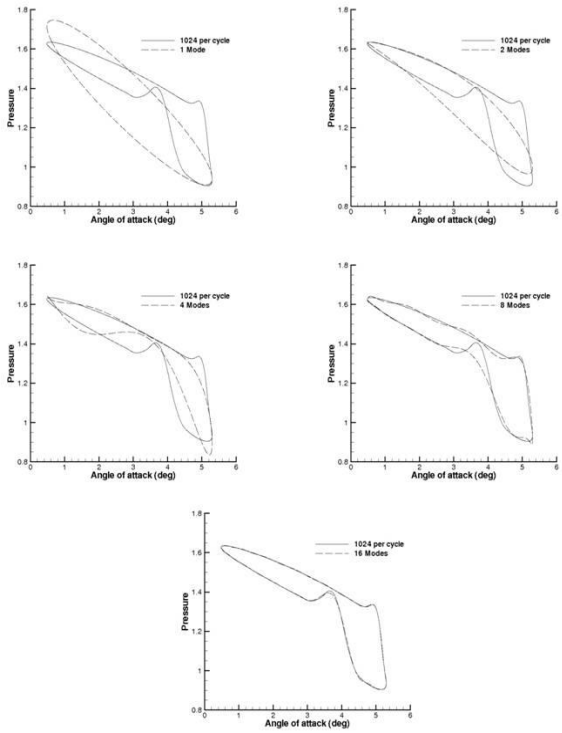

Figure 24: Pressure versus angle of attack

turbomachinery. For an introduction to the literature on NSV, see [88].

One of the most interesting aspects of buffet is the relatively benign time signatures of the lift (and moment) oscillations on an airfoil or wing. See Figure 21. The lift oscillation is not only periodic, but nearly simple harmonic. Yet this is a result of a nonlinear limit cycle oscillation of the fluid and involves substantial shock oscillations and in at least some cases separated flow. How can this be?

Some years ago, Williams [89] showed using transonic potential flow theory that as the motion of an airfoil or wing becomes small, the shock displacement is linearly proportional to the airfoil or wing motion and the lift and moment (and indeed all generalized forces) are linearly proportional to the airfoil or wing motion. This is a remarkable result because the pressure distribution along the airfoil is highly nonlinear even for small motions if one examines a position on the airfoil over which the shock moves. Williams was able to show these results analytically for the potential flow model and subsequent numerical computations using Euler and Navier-Stokes fluid models have confirmed a similar result.

A recent paper by Woodgate and Badcock [90] has a nice result that graphically illustrates this point for an Euler flow model. At the many points along the airfoil that *are not traversed by the shock motion,* the pressure is nearly harmonic in time as illustrated by the nearly elliptical phase plane plot of pressure versus angle of oscillating motion of the airfoil (not shown here). On the other hand at the points along the airfoil that *are traversed by the shock motion,* the pressure time history although periodic has many higher harmonics as well. These computations were done using a harmonic balance method [3,4] and Woodgate and Badcock show that many higher harmonics are indeed needed to resolve the local pressure time history when the point on the airfoil is traversed by the shock. In Figure 24 results are shown for one, two, four, eight and sixteen harmonics. The good news for the modeling of aeroelastic systems is that the generalized forces including lift and moment do not usually have this higher harmonic content unless the airfoil or wing motions are very large (an effective angle of attack near the stall angle) because of the spatial filtering that occurs due to integration over the airfoil chord or wing area when computing lift, moment and other generalized forces.

VI. Concluding Remarks

Substantial progress has been made in modeling and understanding nonlinear aeroelastic phenomena. Experimental and theoretical investigations have shown good correlation for a number of nonlinear physical mechanisms. As a broad generalization, one may say that our understanding of and correlation among alternative theoretical models and experiment is further advanced for nonlinear structural mechanisms such as freeplay and large deflection geometric nonlinearities of beams and plates, than it is for nonlinear fluid mechanisms such as large shock motions and separated flows. Nevertheless more accurate and much more computationally efficient theoretical models are now becoming available for nonlinear aerodynamic flows and there is cause for optimism in addressing these issues going forward.

As has been emphasized throughout this paper, a number of physical mechanisms can lead to nonlinear aeroelastic response including the impact of static (steady flow) fluid or static structural nonlinearities in changing the flutter boundary of an aeroelastic system. Of course dynamic nonlinearities play a critical role in the development of limit cycle oscillations, hysteresis in flutter and LCO response, and the sensitivity of both to initial and external disturbances.

The good news for the flight vehicle designer is that because of nonlinear aeroelastic effects, finite amplitude oscillations can in some cases replace what would otherwise be the rapidly growing and destructive oscillations of classical flutter behavior. A careful consideration and design of favorable nonlinearities offers a new opportunity for improved performance and safety of valuable wind tunnel models, flight vehicles, their operators and passengers.

Finally and inevitably some important topics have been omitted due to space and time limitations. The insightful article on rotorcraft aeroelasticity by Friedmann [91] is highly recommended; for turbomachinery aeroelasticity, see the authoritative volume edited by Hall, Kielb and Thomas [92] and for an entrée to the literature on morphing aircraft such as the folding wing concept see the paper by Attar et al [93]. The work of Batina [94] on advanced concepts in transonic small disturbance potential flow theory and computation also reminds us that there are still valuable opportunities for significant advances in that field as well.

VII. References

1. Dowell, E. H., Edwards. J.W. and Strganac, T.W, "Nonlinear Aeroelasticity," Journal of Aircraft, Vol. 40, No. 5, Sept.-Oct. 2003, pp. 857-874.

2. Dowell, E. H. and Tang, D. M., "Nonlinear Aeroelasticity and Unsteady Aerodynamics," AIAA Journal, Vol. 40, No. 9, 2002, pp. 1697-1707.

3. Dowell, E. H. and Hall, K. C., "Modeling of Fluid-Structure Interaction," Annual Reviews of Fluid Mechanics, Vol. 33, 2001, pp. 445-490.
4. Lucia, D. J., Beran, P. S. and Silva, W. A., "Reduced-Order Modeling: New Approaches for Computational Physics," Progress in Aerospace Sciences, Vol. 40, No. 1-2: 2004, pp. 51-117.
5. Dowell, E. H., Clark, R., Cox, D., Curtiss, H. C. Jr., Edwards, J. W., Hall, K. C., Peters, D. A., Scanlan, R., Simiu, E., Sisto, F. and Strganac, T. W., "A Modern Course in Aeroelasticity," 4th Edition, Kluwer Academic Publishers, 2004.
6. Dowell, E. H. and Tang, D. M., "Dynamics of Very High Dimensional Systems," World Scientific, 2003. See especially Chapters 4, 13 and 14.
7. Hashimoto, A. , Aoyama, T. and Nakamura, Y., "Effects of Turbulent Boundary Layer on Panel Flutter, " AIAA Journal, Vol. 47, No. 12, 2009, pp. 2785-2791.
8. Dowell, E. H., "Aerodynamic Boundary Layer Effects on Flutter and Damping of Plates," Journal of Aircraft, Vol. 10, No. 12, 1973, pp. 734-738.
9. Muhlstein, L. and Gaspers, P., and Riddle, D. ,"An Experimental Study of the Influence of the Turbulent Boundary Layer on Panel Flutter," NASA TN D4486, 1968.
10. Dugundji, J., Dowell, E. and Perkin, B., "Subsonic Flutter of Panels on a Continuous Elastic Foundation, "AIAA Journal, Vol. 1, No. 5, 1963, pp. 1146-1154.
11. Dowell, E. H., "Aeroelasticity of Plates and Shells, "Kluwer Academic Publishers, 1975. See Appendix II.
12. Tang, D. M., Yamamoto, H. and Dowell, E. H., "Flutter and Limit Cycle Oscillations of Two-Dimensional Panels in a Three- Dimensional Axial Flow, "Journal of Fluids and Structures, Vol. 17, 2003, pp. 225-242.
13. Tang, L., Paidoussis, and Jiang, J. "Cantilevered Flexible Plates in Axial Flow: Energy Transfer and the Concept of a Flutter-Mill," Journal of Sound and Vibration, Vol. 326, 2009, pp. 263-276.
14. Hoffman, N. R., "Subsonic Flutter Model Tests of an All-Movable Stabilizer with 35 Degree Sweepback," WADC Technical Note 55-623. November 1955.
15. Tang, D., Dowell, E. H. and Virgin, L. N., "Limit Cycle Behavior of an Airfoil with a Control Surface," Journal of Fluids and Structures, Vol. 12, No. 7, 1998, pp. 839-858.
16. Tang, D. and Dowell, "Aeroelastic Airfoil with Freeplay at Angle of Attack with Gust Excitation," AIAA Journal, Vol. 48, No. 2, pp. 427-442.
17. Lee, D., Chen, P., Tang, D. and Dowell, E., "Nonlinear Gust Response of a Control Surface with Freeplay," AIAA 2010-3116, presented at the 51st AIAA SDM Conference, April 12-15, Orlando, Fl., 2010.
18. Schlomach, C., "All-Moveable Control Surface Freeplay," presentation to the Aerospace Flutter and Dynamics Council, NASA Langley Research Center, April 2-3, 2009.
19. Lieu, T., Farhat, C. and Lesoinne, A., "Reduced-Order Fluid/Structure Modeling of a Complete Aircraft Configuration," Computer Methods in Applied Mechanics and Engineering, Vol. 195, No. 41-43, 2006, pp. 5730-5742.
20. Lieu, T. and Farhat, C., "Adaptation of Aeroelastic Reduced-Order Models and Application to an F-16 Configuration," AIAA Journal, Vol. 45, No. 6, 2007, pp. 1244-1257.
21. Amsallem, D. and Farhat, C., "Interpolation Method for Adapting Reduced-Order Models and Application to Aeroelasticity," AIAA Journal, Vol. 46, No. 7, 2008, pp. 1803-1813.
22. Romanowski, M. C., "Reduced Order Unsteady Aerodynamic and Aeroelastic Models Using Kahunen-Loeve Eigenmodes [POD Modes], AIAA Paper96-3981, presented at the AIAA/NASA/ISSMO Symposium on Multidisciplinary Analysis and Optimization, Bellevue, Washington, 1996.
23. Hall, K.C., Thomas, J. P. and Dowell, E. H., "Proper Orthogonal Decomposition Technique for Transonic Unsteady Aerodynamic Flows," AIAA Journal, Vol.38, No. 10, 2000, pp. 1853-1862.
24. Thomas, J. P., Dowell, E. H. and Hall, K. C., "Three-Dimensional Aeroelasticity Using Proper Orthogonal Decomposition Based Reduced Order Models," Journal of Aircraft, Vol. 40, No. 3, 2003, pp. 544-551.
25. Dowell, E. H., Thomas, J. P. and Hall, K. C., "Transonic Limit Cycle Oscillation Analysis Using Reduced Order Models," Journal of Fluids and Structures, Vol. 19, No. 1, 2004, pp. 17-27.
26. Beran, P. S., Lucia, D. J. and Pettit, Cl. L., "Reduced-Order Modeling of Limit-Cycle Oscillation for Aeroelastic Systems," Journal of Fluids and Structures, Vol.19, No. 5, 2004, PP. 575-590.
27. Lucia, D. J. and Beran, P. S., "Reduced-Order Model Development Using Proper Orthogonal Decomposition and Volterra Theory," AIAA Journal, Vol. 42, No. 6, 2004, pp. 1181 -1190.
28. Mortara, S. A., Slater, J. and Beran, P., "Analysis of Nonlinear Aeroelastic Panel Response Using Proper Orthogonal Decomposition," Journal of Vibration and Acoustics, Vol. 126, No. 3, 2004, pp. 416-421.
29. Anttonen, J. S. R., King, P. I. and Beran, P. S., "Applications of Multi-POD to a Pitching and Plunging Airfoil," Mathematical and Computer Modeling," Vol.42, No. 3-4, 2005, pp. 245-259.

30. McMullen, M. and Jameson, A., "The Computational Efficiency of Non-linear Frequency Domain Methods," Journal Computational Physics, Vol. 212, No. 2, 2006, pp. 637-661.
31. McMullen, M., Jameson, A. and Alonzo, J., "Demonstration of Nonlinear Frequency Domain Methods," AIAA Journal, Vol. 44, No. 7, 2006, pp. 1428-1435.
32. Timme, S. and Badcock, K., "Implicit Harmonic Balance Solver for Transonic Flow with Forced Motions," AIAA Journal, Vol. 47, No. 4, 2009, pp. 893-901.
33. Hall, K. C., Thomas, J. P. and Clark, W. S., "Computation of Unsteady Nonlinear Flows in Cascades Using a Harmonic Balance Technique," AIAA Journal, Vol. 40, No. 5, 2002, pp. 879-886.
34. Thomas, J. P., Dowell, E. H. and Hall, K. C., "Modeling Viscous Transonic Limit Cycle Oscillations Behavior Using a Harmonic Balance Approach," Journal of Aircraft, Vol. 41, No. 6, 2004, pp. 1266-1274.
35. Beran, P. S. and Lucia, D. J., "A Reduced Order Cyclic Method for Computation of Limit Cycles," Nonlinear Dynamics, Vol. 39, No. 1-2, 2005, pp. 143-158.
36. Liu, L., Thomas, J. P., Dowell, E. H., Attar, P. J. and Hall, K.C., "A Comparison of Classical and High Dimensional Harmonic Balance Approaches for a Duffing Oscillator," Journal of Computational Physics, Vol. 215, No. 1, 2006, pp. 298-320.
37. Dowell, E. H., Hall, K. C., Thomas, J. P., Kielb, R. E., Spiker, M. A. and Denegri, Jr., C. M., "A New Solution Method for Unsteady Flows Around Oscillating Bluff Bodies," Proceedings of the IUTAM Symposium on Fluid-Structure Interaction in Ocean Engineering, 2007, Springer.
38. Custer, C. H., Thomas, J. P., Dowell, E. H. and Hall, K. C., "A Nonlinear Harmonic Balance Method for the CFD Code OVERFLOW 2," International Forum on Aeroelasticity and Structural Dynamics, Paper 2009-050, Seattle, Washington, June 2009.
39. Thomas, J. P., Custer, C. H., Dowell, E. H. and Hall, K. C., "Unsteady Flow Computations Using a Harmonic Balance Approach Implemented about the OVERFLOW 2 Flow Solver," 19th AIAA Computational Fluid Dynamics Conference, Paper 2009-4270, San Antonio, Texas, June 2009.
40. Thomas, J. P., Dowell, E. H. and Hall, K. C., "Using Automatic Differentiation to Create Nonlinear Reduced Order Model Aerodynamic Solver," AIAA Journal, Vol. 48, No. 1, 2010, pp. 19-24.
41. Thompson, J. M. T. and Stewart, H. B., Nonlinear Dynamics and Chaos, John Wiley and Sons, 1988.
42. Denegri, C.M., Jr., "Correlation of Classical Flutter Analyses and Nonlinear Flutter Responses Characteristics," International Forum on Aeroelasticity and Structural Dynamics, pp. 141-148, Rome, Italy, June 1997.
43. Denegri, C.M., Jr. and Cutchins, M.A., "Evaluation of Classical Flutter Analysis for the Prediction of Limit Cycle Oscillations," AIAA Paper 97-1021, April 1997.
44. Denegri, C.M., Jr., "Limit Cycle Oscillation Flight Test Results of a Fighter with External Stores," Journal of Aircraft, Vol. 37, No. 5, 2000, pp. 761-769.
45. Denegri, C.M., Jr. and Johnson, M.R., "Limit Cycle Oscillation Prediction Using Artificial Neural Networks," Journal of Guidance, Control, and Dynamics, Vol. 24, No. 5, 2001, pp. 887-895.
46. AGARD Specialists Meeting on Wings-with-Stores Flutter, 39th Meeting of the Structures and Materials Panel, AGARD Conference Proceedings No. 162, Munich, Germany, October 1974.
47. Bunton, R.W. and Denegri, C.M. Jr., "Limit Cycle Oscillation Characteristics of Fighter Aircraft," Journal of Aircraft, Vol. 37, No. 5, 2000, pp. 916-918.
48. Cunningham, A.M. Jr., "A Generic Nonlinear Aeroelastic Method with Semi-Empirical Nonlinear Unsteady Aerodynamics," Vol. 1 and 2, AFRL-VA-WP-R-1999-3014, 1999.
49. Cunningham, A.M., Jr., "The Role of Nonlinear Aerodynamics in Fluid-Structure Interactions," AIAA Paper 98-2423, 1998.
50. Cunningham, A.M., Jr. and Geurts, E.G.M., "Analysis of Limit Cycle Oscillation/Transonic High Alpha Flow Visualization," AFRL-VA-WP-TR-1998-3003, Part I, January 1998.
51. Dobbs, S.K., Miller, G.D. and Stevenson, J.R., "Self Induced Oscillation Wind Tunnel Test of a Variable Sweep Wing," 26th AIAA/ASME/ASCE/AHS Structures, Structural Dynamics and Materials Conference, AIAA Paper 85-0739-CP, Orlando, FL, April 15-17, 1985.
52. Hartwich, P.M., Dobbs, S.K., Arslan, A.E. and Kim, S.C., "Navier-Stokes Computations of Limit Cycle Oscillations for a B-1-Like Configuration," AIAA Paper 2000-2338, AIAA Fluids 2000, Denver, CO, June 2000.
53. Dreim, D.R., Jacobson, S.B. and Britt, R.T., "Simulation of Non-Linear Transonic Aeroelastic Behavior on the B-2," NASA CP-1999-209136, CEAS/AIAA/ICASE/NASA Langley International Forum on Aeroelasticity and Structural Dynamics, pp. 511-521, June 1999.
54. Croft, J., "Airbus Elevator Flutter: Annoying or Dangerous?", Aviation Week and Space Technology, August 2001.

55. Dowell, E.H., "Aeroelasticity of Plates and Shell," Kluwer Academic Publishers, 1975.
56. Dowell, E. H., "Panel Flutter," NASA Special Publication, SP-8004, 1972.
57. Yurkovich, R.N., Liu, D.D. and Chen, P.C., "The State-of-the-Art of Unsteady Aerodynamics for High Performance Aircraft," AIAA Paper 2001-0428, Aerospace Sciences Conference, January 2001.
58. Bennett, R.M. and Edwards, J.W., "An Overview of Recent Developments in Computational Aeroelasticity," AIAA Paper No. 98-2421, presented at the AIAA Fluid Dynamics Conference, Albuquerque, NM, June 1998.
59. Farhat, C. and Lesoinne, M., "Enhanced Partitioned Procedures for Solving Nonlinear Transient Aeroelastic Problems," AIAA Paper 98-1806, April 1998.
60. Raveh, D.E., Levy, Y. and Karpel, M., "Efficient Aeroelastic Analysis Using Computational Unsteady Aerodynamics," Journal of Aircraft, Vo. 38, No. 3, 2001, pp. 547-556.
61. Thomas, J.P., Dowell, E.H. and Hall, K.C., "Three-Dimensional Transonic Aeroelasticity Using Proper Orthogonal Decomposition Based Reduced Order Models," AIAA Paper 2001-1526, presented at 42nd AIAA/ASME/ASCE/AHS/ ASC Structures, Structural Dynamics, and Materials Conference and Exhibit, Seattle, WA, April 16-19, 2001.
62. Gupta, K.K., "Development of a Finite Element Aeroelastic Analysis Capability," Journal of Aircraft, Vol. 33, No. 5, 1996, pp. 995-1002.
63. Scott, R.C., Silva, W.A., Florance, J.R. and Keller, D.F., "Measurement of Unsteady Pressure Data on a Large HSCT Semi-span Wing and Comparison with Analysis," AIAA Paper 2002-1648.
64. Silva, W.A., Keller, D.F., Florance, J.R., Cole, S.R. and Scott, R.C., "Experimental Steady and Unsteady Aerodynamic and Flutter Results for HSCT Semi-span Models," 41st Structures, Structural Dynamics and Materials Conference, AIAA No. 2000-1697, April 2000.
65. Bennett, R.M., Eckstrom, C.V., Rivera, J.A., Jr., Danberry, B.E., Farmer, M.G. and Durham, M.H., "The Benchmark Aeroelastic Models Program: Description and Highlights of Initial Results," NASA TM 104180, April 1991.
66. Bennett, R.M., Scott, R.C., and Wieseman, C.D., "Computational Test Cases for the Benchmark Active Controls Model," Journal of Guidance, Control, and Dynamics, Vol. 23, No. 5, September 2000, pp. 922-929.
67. Kholodar, D.E., Dowell, E.H., Thomas, J.P., and Hall, K.C., "Limit-Cycle Oscillations of a Typical Airfoil in Transonic Flow," Journal of Aircraft, Vol. 41, No. 5, AIAA, 2004.
68. Rivera, Jr., J., "Dansberry, B., Bennett, R., Durham, M., and Silva, W., "NACA0012 Benchmark Model Experimental Flutter Results with Unsteady Pressure Distributions," Technical Memorandum 107581, NASA, 1992.
69. Schwarz, J.B., Dowell, E.H., Thomas, J.P., Hall, K.C., Rausch, R.D. and Bartels, R.E., "Improved Flutter Boundary Prediction for an Isolated Two Degree of Freedom Airfoil", Journal of Aircraft, Vol. 46, No. 6, , 2009, pp. 2069-2076.
70. Thomas, J.P., Dowell, E.H., and Hall, K.C., "Theoretical Predictions of Limit Cycle Oscillations for Flight Flutter Testing of the F-16 Fighter," Journal of Aircraft, Vol. 46, No. 5 , 2009, pp. 1667-1672.
71. Dowell, E.H. and Tang, D., "Nonlinear Aeroelasticity and Unsteady Aerodynamics," AIAA Journal, Vol. 40, No. 9, 2002, pp. 1697-1707.
72. Gordnier, R.E. and Melville, R.B., "Physical Mechanisms for Limit-Cycle Oscillations of a Cropped Delta Wing," AIAA Paper 99-3796, Norfolk, VA, June 1999.
73. Gordnier, R.E. and Melville, R.B., "Numerical Simulation of Limit-Cycle Oscillations of a Cropped Delta Wing Using the Full Navier-Stokes Equations," International Journal of Computational Fluid Dynamics, Vol. 14 No. 3, 2001, pp. 211-224.
74. Schairer, E.T. and Hand, L.A., "Measurement of Unsteady Aeroelastic Model Deformation by Stereo Photogrammetry," AIAA Paper 97-2217, June 1997.
75. Thomas, J. P., Dowell, E. H. and Hall, K. C., "A Harmonic Balance Approach for Modeling Three-Dimensional Nonlinear Unsteady Aerodynamics and Aeroelasticity," IMECE-2002-32532, Presented at the ASME International Mechanical Engineering Conference and Exposition, November 17-22, 2002, New Orleans, Louisiana.
76. Edwards, J.W., "Calculated Viscous and Scale Effects on Transonic Aeroelasticity," Paper No. 1 in "Numerical Unsteady Aerodynamic and Aeroelastic Simulation". AGARD Report 822, March 1998.
77. Edwards, J.W., Schuster, D.M., Spain, C.V., Keller, D.F. and Moses, R.W., "MAVRIC Flutter Model Transonic Limit Cycle Oscillation Test," AIAA Paper No. 2001-1291, April 2001.
78. Edwards, J.W., "Transonic Shock Oscillations and Wing Flutter Calculated with an Interactive Boundary Layer Coupling Method," NASA TM-110284, August 1996.

79. Parker, E.C., Spain, C.V. and Soistmann, D.L., "Aileron Buzz Investigated on Several Generic NASP Wing Configurations," AIAA Paper 91-0936, April 1991.
80. Pak, C. and Baker, M.L., "Control Surface Buzz Analysis of a Generic Nasp Wing," AIAA Paper 2001-1581, 2001.
81. Huttsell, L., Schuster, D., Volk, J., Giesing, J. and Love, M., "Evaluation of Computational Aeroelasticity Codes for Loads and Flutter," AIAA Paper 2001-569, 2001.
82. Edwards, J. W., "Calculated Viscous and Scale Effects on Transonic Aeroelasticity," Journal of Aircraft, Vol. 45, No. 6, 2008, pp. 1863-1871.
83. Barakos, G. and Drikakis, D., "Numerical Simulation of Transonic Buffet Flows Using Various Turbulence Closures, "International Journal of Heat and Fluid Flow, Vol. 21, 2000, pp. 620-626.
84. Raveh, D., "A Numerical Study of an Oscillating Airfoil in Transonic Buffeting Flows, " AIAA Journal, Vol. 47, No. 3, 2009, pp. 505-515.
85. Raveh, D. and Dowell, E. H., "Aeroelastic Response of Airfoil in Buffeting Transonic Flows," In International Forum on Aeroelasticity and Structural Dynamics, Seattle, WA, 2009, IFASD-2009-161.
86. Raveh, D. and Dowell, E. H., "Frequency Lock-In Phenomenon for Oscillating Airfoils in Buffeting Flows," Accepted for publication in the Journal of Fluids and Structures.
87. McDevitt, J. B. and Okuno, A. F., "Static and Dynamic Pressure Measurements on a NACA 0012 Airfoil in the Ames High Reynolds Number Facility," NASA TP 2485, 1985.
88. Kielb, R., Barter, J. T. and Hall, K. C., "Blade Excitation by Aerodynamic Instabilities-A Compressor Blade Study," ASME GT-2003-38634, ASME Turbo Expo Conference, 2003.
89. Williams, M. H., "Linearization of Unsteady Transonic Flows Containing Shocks," AIAA Journal, Vol. 17, No. 4, 1979, pp.394-397.
90. Woodgate, M. A. and Badcock, K. J., "Implicit Harmonic Balance Solver for Transonic Flow with Forced Motions," AIAA Journal, Vol. 47, No. 4, 2009, pp. 893-901.
91. Friedmann, P.O., "Rotary-Wing Aeroelasticity: Current Status and Future Trends," AIAA Journal, Vol. 42, No. 10, 2004, pp. 1953-1972.
92. Hall, K.C., Kielb, R.E., Thomas, J.P., editors, "Unsteady Aerodynamic, Aeroacoustics and Aeroelasticity of Turbomachines," Proceedings of the 10th International Symposium held at Duke University, 8-11 September, 2003, Springer, 2006.
93. Attar, P., Tang, D. and Dowell, E. H., "Nonlinear Aeroelastic Study for Folding Wing Structures, " Presented at the NATO AVT-168 Symposium on Morphing Structures, 2009.
94. Batina, J., Introduction of the ASP3D Computer Program for Unsteady Aerodynamics and Aeroelastic Analyses, NASA TM-2005-213909, 2005.